

A&A manuscript no.  
(will be inserted by hand later)

Your thesaurus codes are:  
( )

# Models for the interpretation of CaT and the blue Spectral Indices in Elliptical Nuclei

M. Mollá,<sup>1</sup> and M.L. García-Vargas<sup>2</sup>

<sup>1</sup> Departement de Physique, Université Laval, Chemin St-Foy, G1K 7P4-Quebec, Canada \*

<sup>2</sup> Instituto de Astrofísica de Canarias, GRANTECAN Project, Vía Láctea S/N. 38200 La Laguna, Tenerife. Spain

Received xxxx 2000; accepted xxxx 2000

**Abstract.** We present a grid of theoretical models where the calculation of absorption line spectral indices in both the blue and red wavelength ranges is done with the same evolutionary synthesis code. We have computed some of these indices: CaT, Na I, Mg I in the near infrared and Mgb, Mg<sub>2</sub>, Fe52, Fe53, NaD and H $\beta$ , in the blue-visible range, for Single Stellar Population (SSP) of 6 different metallicities, (Z=0.0004, 0.001, 0.004, 0.008, 0.02 and 0.05), and ages from 4 Myr to 20 Gyr.

From the comparison of these evolutionary synthesis models with a compilation of elliptical galaxy data from the literature, we find that the observed CaT index follows the blue  $\langle\text{Fe}\rangle$  index rather than Mg<sub>2</sub> as the models predict. If this implies an *over-abundance* [Mg/Ca] and we take into account the masses of stars which produce Mg and Ca, these stars could form in a time scale shorter than 5 Myr from the beginning of the star formation process. Alternatively, an IMF biased towards very massive stars ( $M > 40M_{\odot}$ ) at the early epoch of star formation in elliptical nuclei has to be assumed. We also suggest to revise the calculation of the nucleosynthesis yield of Magnesium.

By using the diagnostic diagram CaT-H $\beta$  to disentangle age and metallicity in such populations, we obtain around solar abundances and a sequence of ages between 4 and 16 Gyr for the galaxy sample.

**Key words:** Calcium Triplet – Elliptical galaxies

## 1. Introduction

The study of chemical abundances in elliptical galaxies has traditionally been performed through the analysis of absorption features usually present in their spectra (see the recent review by Henry & Worthey 1999). The observation of such indices in the blue spectral range—in particular the so called *Lick* indices—has been a very fruitful tool to interpret the physical properties of elliptical

galaxies and globular clusters, both assumed to consist of old stellar populations. There are many articles compiling observational data for some of these indices (e.g. Trager et al. 1998 and references therein), specially in Mg<sub>2</sub> and  $\langle\text{Fe}\rangle = (\text{Fe}5270 + \text{Fe}5335)/2$ . Some works have also measured other indices in the same spectral region such as Mgb, NaD and H $\beta$ .

Evolutionary synthesis models are the tool most frequently used to interpret observed spectra. There are a large number of different models (see Leitherer et al. 1998, and references therein) which have become available thanks to the development of theoretical isochrones, computed for a wide range of ages and metallicities. An additional basic input for these models is an atlas of stellar spectra (empirical or theoretical) which provides the spectral energy distribution of each elemental area of the Hertzsprung-Russell Diagram (HRD). If the spectral resolution of the available stellar atlas is good enough, line-strength indices can be measured directly in the final spectrum resulting from the calculation (see Vazdekis 1999).

When this is not the case, or when the stellar atlas consists of atmosphere models, empirical calibrations of line-strength indices (also known as *fitting functions*) must be incorporated into the models. These fitting functions are obtained by observing a large sample of stars covering the widest available range of the basic atmospheric stellar parameters (effective temperature  $T_{\text{eff}}$ , surface gravity  $\log g$ , and metallicity—usually parameterized by [Fe/H]—; some authors also include relative abundances [X/Fe] parameters to introduce elemental ratios different from solar). Among the most employed sets of fitting functions are those provided by the Lick group (Gorgas et al. 1993; Worthey et al. 1994—hereafter WFG94), and those of the Marseille group (Idiart & Freitas-Pacheco 1995, Borges et al. 1995; hereafter BIFT95). Examples of evolutionary synthesis models, in which blue spectral indices for single stellar populations (SSP) of different ages and metallicities are computed, are those of Worthey (1994, hereafter W94), Casuso et al. (1996), Bressan et al. (1996, hereafter BCT96), Vazdekis et al. (1996 hereafter VCPB96), and Kurth et al. (1999, hereafter KFF99). All these works have employed the polynomial functions of

*Send offprint requests to:* Mercedes Mollá

\* *Present Address:* Dep. de Física Teórica, Universidad Autónoma de Madrid, 28049 Cantoblanco, Madrid, Spain

*Correspondence to:* mercedes@pollux.ft.uam.es

WFGB94. On the other hand, BIFT95 have made use of their own set of fitting functions, which have also been employed in the models of Tantalo et al. (1998). Most of these synthesis models give estimates for the blue-yellow line-strength indices, such as  $Mgb$ ,  $Mg_2$ ,  $Fe5270$  and  $Fe5335$  (sometimes only  $\langle Fe \rangle$ ),  $NaD$  and  $H\beta$ .

An important result is obtained from the study of the locus of data in the plane  $Mg_2$ - $Fe$  (where  $Fe$  means an iron index such as  $Fe5270$ ,  $Fe5335$  or  $\langle Fe \rangle$ ). The correlation followed by globular cluster data is adequately reproduced by synthetic models of spectral indices applied to old stellar populations of low metallicities, a result which is not unexpected, since most of the poor-metal stars used to calibrate the spectral index dependence on metallicity are members of these globular clusters. This correlation is steeper than that found for elliptical galaxy nuclei which cannot be fitted by the models even by using the oldest and more metal-rich stellar populations (Burststein et al. 1984; Gorgas et al. 1990; Worthey et al. 1992; Davies et al. 1993; Carollo & Danzinger 1994, 1994b; Fisher et al. 1996; Vazdekis et al. 1997). In fact, elliptical galaxies are located below the lines in the mentioned diagrams. The usual explanation states that old elliptical galaxies formed stars very quickly in the past, after the production of large quantities of magnesium and other elements by massive stars (through the ejection of metals by Type II supernovae, SNe), but before the bulk of iron production, which is mainly synthesized by Type I supernovae resulting from the evolution of low-mass stars. The iron-peak elements appear at least 1 Gyr later than the  $\alpha$ -elements in the interstellar medium. This result limits the star formation duration to less than 1 Gyr, after the start of the process

Therefore, the so-called *over-abundance* of Magnesium over Iron is actually an *under-abundance* of Iron, in terms of the absolute values of total abundances, and since Calcium is also an  $\alpha$ -element, it should be expected that Ca indices follow the  $Mg_2$  behavior: if CaT and  $Mg_2$  indices were directly related to the abundances of Calcium and Magnesium, and both elements were mostly produced by Type II SNe, one should expect that a large Mg enrichment would also imply a large proportion of Ca in comparison with the Iron abundance, implying  $[Ca/Fe] > 0$ , too. On the contrary, if models are not able to reproduce the observational data, a new explanation should be proposed. However, elliptical galaxies data seem to follow the model predictions in the  $Ca4455$ - $\langle Fe \rangle$  plane (Worthey 1998) thus implying a  $[Ca/Fe] = 0$ . Since this result is not well understood, here we propose the use of the Calcium Triplet index at  $\sim \lambda 8600 \text{ \AA}$ , CaT ( $\lambda 8542+8662 \text{ \AA}$ ), to test the predictions of theoretical models against observational data in the plane CaT- $\langle Fe \rangle$ . This point will be discussed in detail in the following sections.

It is important to stress that model predictions used to compare the variation of the CaT with other spectral features in the blue spectral region should be obtained

with the same computational technique and inputs, i.e., the same models with identical stellar tracks and atlases of Stellar Energy Distributions, SEDs. For this reason, in this paper we will present index predictions obtained with a revised version of the evolutionary synthesis models already presented by García-Vargas et al. (1998, hereinafter Paper I). There we modeled the equivalent width of the two main lines of the CaII Triplet ( $\lambda 8542, 8662 \text{ \AA}$ ), following the index definition given by Díaz et al. (1989, hereafter DTT), for SSPs with ages ranging from 1 Myr to 17 Gyr, and for 4 different metallicities  $Z=0.004, 0.008, 0.02$  and  $0.05$ . An important conclusion derived from Paper I is that the CaT index is almost constant with age, and only dependent on metallicity for ages older than 1 Gyr, when the IR flux is dominated essentially by giants. This result indicates that the CaT is a potential tool, in conjunction with other age-sensitive indices such as  $H\beta$ , to confront the well-known age-metallicity degeneracy problem in old populations. In fact, both indices produce a quasi-orthogonal grid of constant age and metallicity lines (see Fig. 7 in Paper I). In the revised version of the models employed in this work, we have included the computation of the most common indices in the blue spectral region, following the same strategy as that employed in Paper I for the near-IR indices.

In order to check our model results about CaT in that work, we compared the predicted indices with the globular cluster data (see paper I), and obtained a dependence of this CaT for the oldest stellar populations on the metallicity similar to that estimated from those data. Unfortunately, there were just a few CaT observations in elliptical galaxies to compare with the model results. In this new piece of work we have compiled data for a sample of elliptical galaxies, for which both the CaT and Lick indices are available in the literature. This will allow us to compare the predictions of the new models with the indices measured in both blue and near-IR spectral regions.

This paper is organized in the following way: in Section 2 we give a description of the evolutionary synthesis model, with special attention to changes introduced with respect to Paper I, and we discuss the criteria followed to select the fitting functions. The comparison of models with data is shown in Section 3. A discussion is performed in Section 4 and finally, our conclusions are presented in Section 5.

## 2. The evolutionary synthesis model

### 2.1. Model description

The evolutionary synthesis models presented in this paper have been computed using the technique already described in paper I. The total mass of every SSP is  $1 \times 10^9 M_\odot$  with a Salpeter-type IMF,  $\Phi(m) = m^{-\alpha}$ , with  $\alpha = 2.35$ , from  $m_{low} = 0.6 M_\odot$  to  $m_{up} = 100 M_\odot$ . We have followed the passive evolution of a single-burst stellar population

(SSP) through ages from 4 Myr to 20 Gyr (with a logarithmic age step of 0.1 dex until 10 Gyr, and 0.02 dex afterwards). This wide range is useful to analyze composite populations, as it occurs in spiral disks (see Mollá et al. 2000) or the non-negligible possibility —non treated here— of having recent star formation over-imposed over an older stellar population (see Pellerin & Robert, 1999). In particular it might be used for studying, in the near future, starburst galaxies where the star formation bursts were provoked by radial flows in spiral disks which pushed the gas towards their centers. Thus, this work also is useful to check that this model gives reasonable spectral indices for SSP before applying it to other more complex stellar populations.

The spectral energy distribution for each SSP is synthesized by adding the spectra corresponding to all the points in the theoretical HR diagram, taken from Bressan et al. (1993). The spectrum associated to each point was selected using the closest atmosphere model in the stellar parameter space, and properly luminosity scaled (see García-Vargas et al. 1995). Atmosphere models were taken from Lejeune et al. 1997, 1998, who provide an extensive and homogeneous grid of low-resolution theoretical flux distributions for a large range in  $T_{\text{eff}}$  (from 2000 K to 50000 K), gravity ( $-1.02 < \log g < 5.50$ ), and metallicity ( $-5.0 \leq [M/H] \leq +1.0$ ), by including M dwarf model spectra. We chose their corrected fluxes, color-calibrated flux distributions, constructed through empirical effective temperature-color relations. These spectra span from 91 Å to 16000 nm, with an average spectral resolution of 20 Å in the optical range. In order to provide predictions for the youngest stellar populations, we supplemented the above data with hot stars ( $T_{\text{eff}} > 50000$  K) from Clegg & Middlemass (1987). These last stars do not exist in old stellar populations but they will be necessary in spiral disk models, where young stars usually contribute to the total flux.

The present models have allowed us to compute the evolution of several line-strength indices: Na I, Mg I and CaT in the near-IR, and Mgb,  $Mg_2$ , Fe5270, Fe5335, NaD and H $\beta$  in the blue band. The index definitions given by DTT have been used for the CaT and Mg I indices, whereas the Na I index was computed as in Zhou (1991). The index definitions for the blue indices (Lick/IDS system) can be found in Trager et al. (1998). Although in the comparison with observational data we are only using CaT,  $Mg_2$ ,  $\langle Fe \rangle$  and H $\beta$ , the calculation of the additional indices allow to us to check whether our blue model predictions are compatible with those obtained by other authors. In addition, the Mg I and Na I indices in the near-infrared are predictions which may be useful in the comparison with high-resolution spectral data in low velocity dispersion objects.

To calculate the synthetic line-strength indices, as a function of age and metallicity, we have followed the procedure explained in paper I. The Lick/IDS indices have been computed using two different sets of fitting functions: (1)

the polynomial functions from WFGB94, and (2) the fitting functions from BIFT95. Both sets of formulae give the behavior of each index as a function of the main stellar parameters: gravity, effective temperature, and metallicity or iron abundance [Fe/H]. The BIFT95 functions allow one to include the dependence on  $\alpha$ -element abundance ratios, although in this paper we have assumed  $[\alpha/Fe] = 0.0$ .

Although the CaT was already synthesized in paper I, we have decided to recompute it here in order to consider the differences in the  $m_{\text{low}}$  (we have employed  $0.6 M_{\odot}$ , instead of  $0.8 M_{\odot}$ ), and in the atmosphere models, which now include M dwarf spectra. Thus, this recalculation provides us with a set of indices obtained with the same computational technique. The only difference between the blue and the near-IR indices presented in this paper resides on the stellar libraries used to derive the corresponding indices values. The inclusion of the CaT in the models has been performed by using the predictions, based on model atmospheres, from Jørgensen et al. (1992, hereafter JCJ92). These authors give the equivalent width of the two strongest calcium lines as a function of the stellar effective temperature, surface gravity, and calcium abundance, and when these functions are used for the DTT stellar library, the predictions are in excellent agreement with the data. Thus, we prefer to use JCJ92 models, which revealed a complex behavior of the calcium lines, instead of relations from DTT, who only gave empirical relations between CaT and the stellar parameters, as a first component analysis, in order to explain the parametric behavior of the star sample.

It is very important to highlight that, since JCJ92 predictions are only valid in the temperature range from 4000 to 6600 K, we have extrapolated their fitting functions for cooler stars (see also paper I). Although this is always dangerous, we are confident in the generic trend of JCJ92 results with  $T_{\text{eff}}$ , because these relations, extrapolated for  $T_{\text{eff}} < 4000$  K, were already compared with M stars data in Paper I: a decreasing of CaT with  $T_{\text{eff}}$  was found in both cases. To strengthen our confidence on this point, we show in Fig. 1 the CaT- $T_{\text{eff}}$  relations obtained with the JCJ92 extrapolated functions for different gravities (solid lines), and compare them to CaT data for the cool star samples from Zhou (1991), Mallik (1997) and Zhu et al. (1999). The two first sample data are shown with symbols representing the stellar gravity. The last set data are solid dots. The dotted line is the least squares fit for these data, given by the equation:

$$CaT = 3.2510^{-3} \times T_{\text{eff}} - 4.10 \quad (1)$$

The dependence of the CaT on  $T_{\text{eff}}$  has a similar slope in both, empirical and theoretical, cases. Data are limited by the extrapolation lines for  $\log g = 0.5$  and  $\log g = 2$ . Those with lower gravities seem to be located higher in the graph than those with higher gravities which are lower, by following the same trend than theoretical models. Maybe

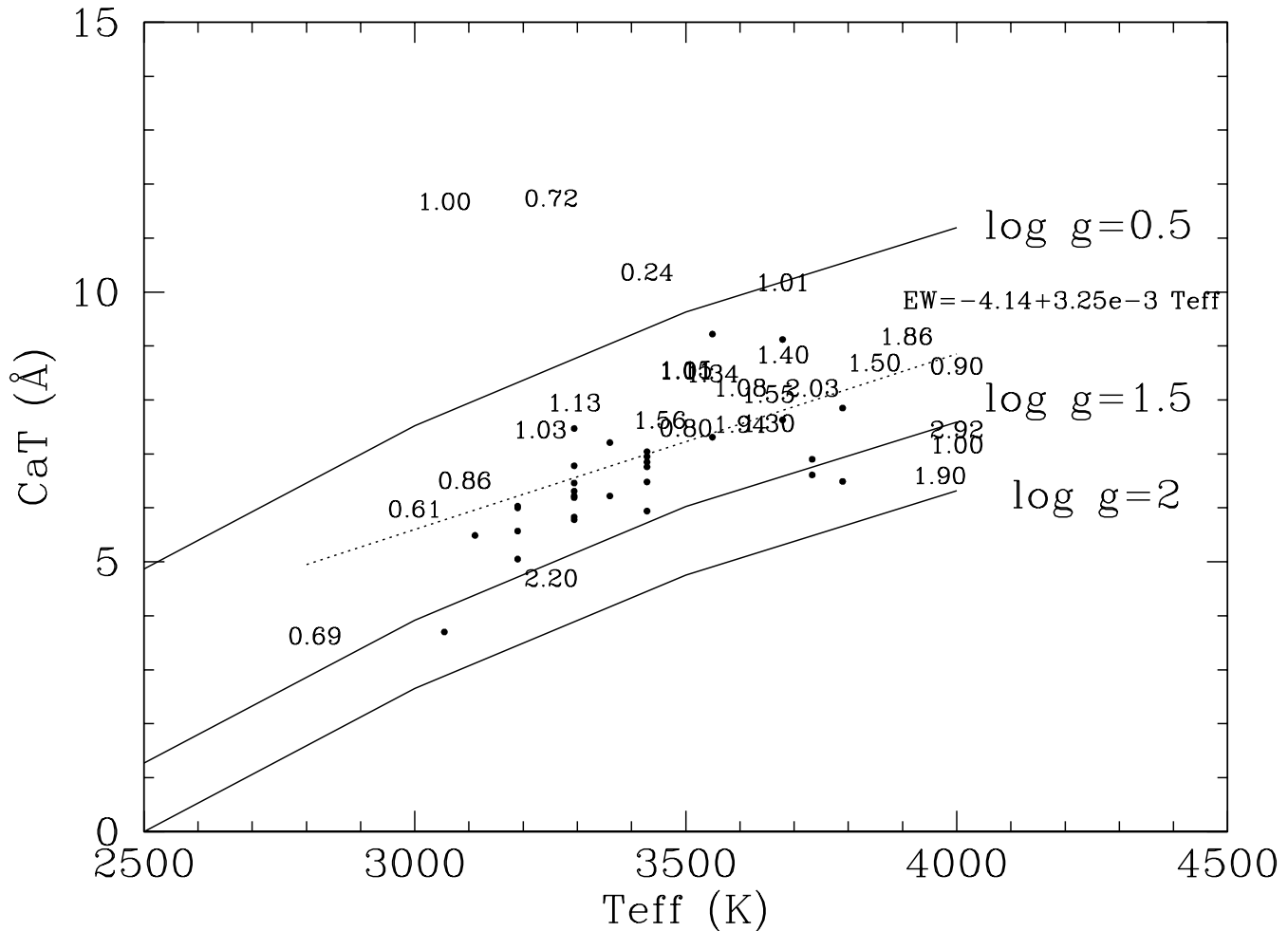


**Fig. 1.** The dependence of CaT with Teff for cool stars. Solid lines represent the extrapolation of the JCJ92 functions for three different gravities given in the figure. Numbers are data, given with symbols as gravity values, from Zhou (1991 1991) and Mallik (1997 1997) Solid dot are data from Zhu et al (1999 1999). The dotted line is the least squares fit to all these data.

the dependence of this theoretical function on gravity does not exactly reproduce the observed one for cool stars, but this point cannot be estimated with the small number of stars with known gravities used for our fit. The influence of using one or the other kind of dependence (empirical equation (1) vs JCJ92 functions) for cool stars on model results will be analyzed in the following section. In summary, this being the main source of uncertainty of the present models, we attempt to use the most adequate solution until more confident fitting functions in this spectral range are available.

For Mg I index, the empirical calibration obtained from DTT have been used, whereas in the case of the Na I index we have followed Equations 3 and 5 from Zhou (1991) who calibrated this index as a function of gravity, stellar abundance and (R-I) Johnson-system color for spectral types from G0 to M3. For the coolest stars we assign a

value of  $1\text{\AA}$ , following data shown by Z91 in their Figure 6. The (R-I) color has been taken from isochrones.

## 2.2. Model Results

Table 1 shows the line-strength predictions for three different metallicities and six age steps, using WFGB94 fitting functions. We have selected these ages since the discussion in this paper is focused on old populations in elliptical galaxies. (The whole set of results for six metallicities and ages from  $\log \text{age} = 6.60$  to  $\log \text{age} = 10.30$  is available in electronic format).<sup>1</sup>

<sup>1</sup> Complete set of Table 2 is only available in electronic form at CDS via anonymous ftp to cdsarc.u-strasbg.fr (130.79.128.5) or via <http://cdsweb.u-strasbg.fr/Abstract.html>, or upon request to authors

**Table 1.** Spectral indices predicted with the evolutionary synthesis model described in this work (with the WFGB94 fitting functions). We only present results for a selected sample of ages and metallicities. The whole set of index predictions is available in electronic format.

log age (yr)	CaT (Å)	Na I (Å)	Mg I (Å)	Mgb (Å)	Mg <sub>2</sub> (mag)	Fe5270 (Å)	Fe5335 (Å)	NaD (Å)	H $\beta$ (Å)
Z=0.008									
9.30	5.356	0.025	0.612	2.138	0.127	1.937	1.574	1.674	3.130
9.60	5.614	0.058	0.622	2.488	0.145	2.146	1.764	1.830	2.461
9.90	5.826	0.083	0.650	2.907	0.172	2.412	2.000	2.013	1.988
10.08	5.895	0.106	0.650	3.143	0.185	2.507	2.082	2.099	1.804
10.14	5.910	0.111	0.652	3.262	0.192	2.563	2.133	2.135	1.728
10.20	5.922	0.124	0.649	3.308	0.195	2.573	2.138	2.153	1.687
Z=0.02									
9.30	6.815	0.136	0.717	2.556	0.163	2.416	2.152	2.355	2.795
9.60	7.063	0.183	0.752	3.335	0.211	2.823	2.541	2.747	2.041
9.90	7.078	0.240	0.759	3.741	0.235	2.967	2.688	2.950	1.749
10.08	7.108	0.255	0.771	4.058	0.260	3.148	2.864	3.173	1.522
10.14	7.071	0.276	0.767	4.117	0.267	3.181	2.894	3.223	1.468
10.20	7.095	0.277	0.772	4.203	0.274	3.242	2.947	3.294	1.405
Z=0.05									
9.30	8.454	0.560	0.868	3.393	0.224	3.047	2.997	3.406	2.296
9.60	8.475	0.610	0.888	4.231	0.283	3.446	3.408	3.970	1.718
9.90	8.329	0.717	0.876	4.683	0.315	3.627	3.594	4.276	1.435
10.08	8.285	0.766	0.876	4.989	0.342	3.786	3.746	4.568	1.282
10.14	8.300	0.763	0.878	5.081	0.352	3.865	3.810	4.710	1.222
10.20	8.301	0.768	0.878	5.120	0.359	3.909	3.856	4.792	1.179

The results for the CaT index are very similar to those from paper I. As a comparison, for an age of 13 Gyrs and abundances  $Z=0.004$ , 0.008, 0.02 and 0.05, the present models predict the following values: 4.58, 5.91, 7.08 and 8.30 Å, respectively. The corresponding indices in paper I were: 4.65, 5.95, 7.32 and 9.28 Å. These differences are lower than 10%, implying that the new low-mass limit does not have an important effect on the CaT values, although we note a larger difference (1 Å) for  $Z=0.05$  probably due to the effect of including M dwarf spectra in the atlas, which is larger on the metal-rich stellar populations.

These results are also similar to those obtained by other authors, such as Vazdekis et al. (1996), Idiart et al. (1996, hereafter ITFP96), Mayya(1997) or even the most recent ones from Schiavon et al. (1999, hereafter SBB99). The comparison with other models is made in Table 2 where results for two SSP of 1 Gyr and 13 Gyr old, with different metallicities, are shown. In all cases, the CaT is independent of age and very dependent on metallicity, except for the results from VCPB96 for  $Z=0.05$ , which are smaller than the solar abundance ones.

We represent the time evolution of the results of our model and other models for solar metallicities in Fig. 2, in order to determine whether our conclusion about the independence of CaT on age is a general behavior (Mayya's model is not shown because this work is only dedicated

to stellar populations younger than 1 Gyr). We see that our model gives an almost constant index for old stellar populations in agreement with BCPB96 and SBB99, while models from ITFP97, who used their own stellar library and fitting functions, give CaT values slightly increasing with age ( In order to compare with the same kind of definitions we have converted the CaT values from these authors to the system DTT89). When comparing our model with BCPB96's results, (the only authors who calculated red (CaT and Mg I) and blue spectral indices with the same model) we observe that our values of CaT are ( $\sim 1$  Å) smaller. This is due to the different calibration used to calculate the stellar CaT indices: they use DTT while we use the theoretical equations given by JCJ92. The difference between both models is almost the same offset found between the two grids which were computed in Paper I with these two function sets. Mayya (1997) also use JCJ92, at least in part, reaching basically the same behavior with the age for stellar populations younger than 1 Gyr. SBB99 also obtain no dependence on age, although the absolute values for CaT are not given in their work. In conclusion, with the present knowledge about this index we are confident in the behavior goodness for this index.

This independence of age does not depend on the extrapolation performed for the coolest stars: when the empirical equation (1) is used, instead of the theoretical equa-

**Table 2.** Comparison of model predictions for CaT index, obtained by different authors and this work, for SSP's of 1 and 13 Gyr

Model	CaT(Å) (1 Gyr)	CaT(Å) (13 Gyr)
Z = 0.008		
This work	4.59	5.92
VCPB96	6.24	6.87
ITFP96	5.12	6.25
Mayya97	4.00	—
SBB99	—	0.89 (= 6.32)
Z = 0.02		
This work	6.02	7.10
VCPB96	8.32	8.21
ITFP96	6.20	7.33
Mayya97	3.40	—
SBB99	—	1.00 (=7.10)
Z = 0.05		
This work	7.56	8.30
VCPB96	8.40	8.10
ITFP96	6.85	7.98
Mayya97	4.50	—
SBB99	—	1.15 (=8.17)

Note: SBB99 do not give the total CaT in Å but values normalized to the 13 Gyr and solar metallicity. Values of this Table are estimated by using our result for this age and their dependence on metallicity and ages.

tions from JCJ92, we also obtain a constancy of CaT with age, although with a smaller value (6.76 Å vs 7.10 Å— differences lower than 5%— for solar abundance and  $\log age = 10.20$ ). This behavior is explained when the isochrones information is taken into account. When the stellar populations become older their stars are cooler, which decreases their CaT values following Fig. 1. At the same time the influence of these stars on the total flux of the stellar population increases with age. Both effects compensate each other, resulting in a contribution of these cool stars to the flux in the CaT index which remains constant with age.

We have also checked our model results for the blue spectral indices by comparing them with those derived by other authors. Table 3 shows that our predictions are similar to those from W94 and BCT96 when polynomial fitting functions from WFG94 are used. A comparison of the age evolution of the Mg<sub>2</sub> index is shown in Fig. 3. The similarity with BCT96 is not surprising since their input atmosphere models and isochrones are not very different from those employed in this work. Our indices are also close to those from KFF99 calculated with Padova isochrones, although these authors followed a different method to assign the stellar models in the HR diagram. VCPB96 obtain larger values of Mg<sub>2</sub> and lower values of H $\beta$ . The recent estimations of V99, which are obtained without fitting functions by measuring in the final high-resolution synthetic spectra, are also similar to all models although slightly lower.

The agreement between different authors is clear, with the exception of BIFT95, which predicts lower values than all the other works. Note that, even using the same fitting functions as in BIFT95, we are not able to reproduce their line-strength predictions. This not-well understood discrepancy between the BIFT95 results and our results (and those of other works) leads us to choose our predictions obtained with WFG94 fitting functions for the comparison with observational data.

### 3. Data Analysis

#### 3.1. Comparison of Data with Models

With the aim of addressing the behavior of calcium concerning the  $\alpha$ -element overabundance problem, we start by comparing our model predictions for Mg<sub>2</sub> and CaT with the available data. The set of data is shown in Table 4. This index was measured by Terlevich et al. (1990, hereafter TDT90) for a sample of galaxies, with the aim of finding a method to discriminate between active —i.e. with strong star formation— and normal galaxies. Delisle & Hardy (1992, hereafter DH) also estimated the CaT equivalent width for a reduced sample of elliptical and spiral galaxies, but they used an index definition with different bandpasses. In our compilation there are three sources of IR data: 1) the data from TDT90 ; 2) the set taken from DH. These authors have kindly provided us their spectra in order to calculate again the calcium triplet CaT with the same definitions and windows than the first set; 3)

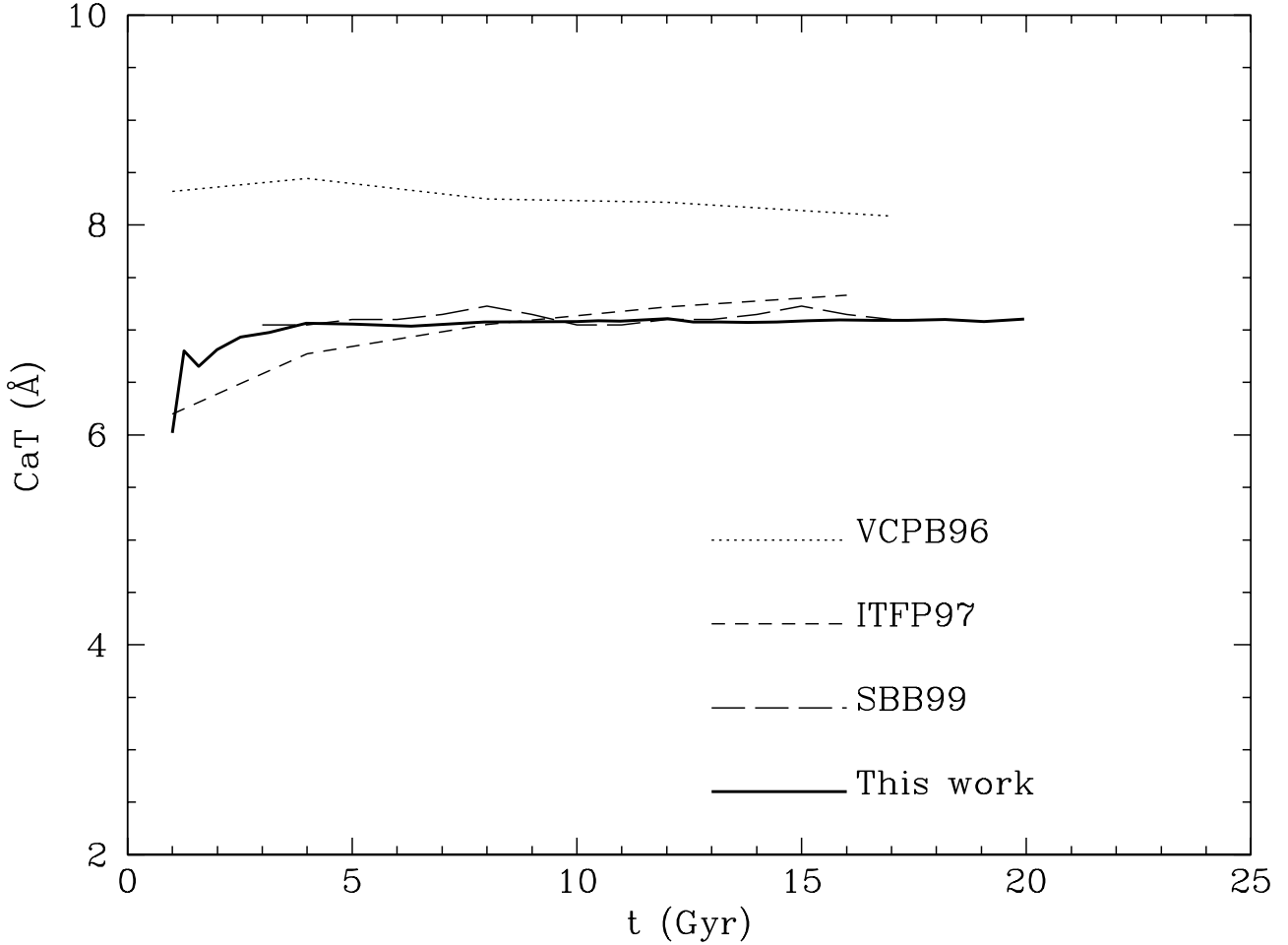


**Fig. 2.** Comparison of the time evolution of the CaT index predicted by SSP models by different authors and this work.

data unpublished from Gorgas et al. (private communication, hereafter GCGV). All these data are in the same measure system. From these sources, we have selected only the galaxies for which blue spectral indices are also available in the literature, following references of column (11). All of them are in the Lick system, therefore we have compiled a uniform set of data. In Column (12) we also show values for  $Mg_2$  as estimated by Davies et al. (1987). These values are systematically lower than those more recent of Column (5).

The measurement of equivalent widths is related to their internal velocity dispersion through the corresponding broadening of the spectral lines which affect both the continuum level and the lines. The effect of the broadening is to decrease the measured EW's (see DTT89, and their fig. 3, where this point was carefully explained). Therefore, the raw data have been corrected, by adding a broadening correction to all of them, and this is how they are shown in the figures. These corrections are lower than the errors

estimated in most of data: for the DTT89 sample, they are  $\sim 0.2\text{\AA}$ , well within the error bars.

We have already discussed that if magnesium and calcium were produced by the same type of massive stars, they should also trace the same mean abundance, in which case the  $[\alpha/Fe]$  overabundance found in E galaxies when studying the Mg lines should also be present in the analysis of the Ca features. We would expect to find all the observational points within the model lines.

This comparison is graphically shown in Fig. 4, where the lines correspond to the model results presented in Table 1: solid lines are isoabundance predictions ( $Z=0.05$ ,  $0.02$  and  $0.008$ , from top to bottom), whereas dashed lines indicate isoages values (ranging from 2 to 16 Gyr, from left to right). Interestingly, model predictions in this diagram indicate that  $Mg_2$  and CaT do not exhibit a strong age-metallicity degeneracy, which means that this index-index plane could be useful for the overabundance study.

**Table 3.** Comparison of model predictions for the line-strength indices in the blue spectral range obtained by different authors and this work, using solar metallicity. Our indices are given for the two choices of fitting functions examined.

Model	Mg <sub>b</sub> (Å)	Mg <sub>2</sub> (mag)	⟨Fe⟩ (Å)	NaD (Å)	H <sub>β</sub> (Å)
Age = 2 Gyr					
W94	2.760	0.189	2.485	2.650	2.752
BCT96	2.607	0.168	2.266	—	2.904
VCPB96	2.056	0.155	2.108	2.292	3.440
V99	2.413	0.150	2.255	—	2.879
KFF99	2.626	0.177	2.365	—	2.722
BIFT95	—	0.089	2.516	1.272	2.676
This work (WFGB94)	2.556	0.163	2.284	2.355	2.795
This work (BIFT95)	2.017	0.144	2.236	1.946	3.136
Age = 10 Gyr					
W94	3.797	0.249	2.890	3.220	1.700
BCT96	3.899	0.255	2.910	—	1.540
VCPB96	3.921	0.261	2.906	3.575	1.491
V99	3.834	0.240	3.000	—	1.710
KFF99	3.789	0.253	2.950	—	1.590
BIFT95	—	0.196	2.960	2.460	1.680
This work (WFGB94)	3.903	0.248	2.908	3.054	1.629
This work (BIFT95)	4.098	0.225	2.927	2.820	1.606
Age = 16 Gyr					
W94	4.129	0.275	3.060	3.560	1.420
BCT96	4.164	0.274	3.060	—	1.350
VCPB96	4.188	0.290	3.141	4.024	1.197
V99	4.071	0.262	3.200	—	1.453
KFF99	4.034	0.274	3.110	—	1.360
BIFT95	—	0.244	3.100	2.980	1.300
This work (WFGB94)	4.203	0.274	3.095	3.294	1.405
This work (BIFT95)	4.856	0.249	3.113	3.075	1.398

It is clear from the figure that, for single populations older than 2 Gyr, the CaT index is roughly constant for a given abundance, as we already explained in the previous section, whereas Mg<sub>2</sub> is sensitive to both age and metallicity.

When the data compiled in Table 4 are plotted in this diagram (using different symbols to distinguish distinct CaT sources, as explained in the plot key), it is apparent that the observed Mg<sub>2</sub> indices spread beyond the model lines. This effect is equivalent to that found by Worthey et al. (1992) in the Mg<sub>2</sub>–⟨Fe⟩ plane. In this figure, we use solid dots to represent the values of Column (12), while the open symbols are those of Column (5). Both kinds of points represent the same galaxies with different estimations of Mg<sub>2</sub>. It is clear that an uncertainty range appears to be involved in the calculation of the index: there exists an offset between Davies et al. (1987) and data from other authors, mostly Gonzalez (1993), models being closer to the observations when the first set is used.

The observed CaT values indicate that the calcium abundance is about solar. Note that the location of data is not dependent on the CaT source (although TDT90 indices show a large abundance scatter, ranging from Z=0.02 to Z=0.05, but some of them are active galaxies).

Another piece of information came from the study of the CaT–⟨Fe⟩ plane, shown in Fig. 5. Model predictions exhibit a larger degeneracy than that observed in Fig. 4. It is important to note, however, that CaT and ⟨Fe⟩ are not completely degenerate due to the dependence of the iron indices on age, almost negligible for the CaT. This result can be easily quantified using the *metal sensitivity* parameter ( $\Delta \log \text{age} / \Delta \log Z$ ) defined by Worthey (1994): for CaT is 134, while for Mg<sub>2</sub> this value is  $\sim 1.8$  and for Fe5270 is  $\sim 2.3$ . It is clear from this calculation that the CaT is an excellent abundance indicator, highly surpassing Fe5709, the iron index most sensitive to metallicity ( $\Delta \log \text{age} / \Delta \log Z = 6.5$ ) in the optical range.

When the observational data set is included in the above plane (see Fig. 5), it is clear that model predictions reproduce the location of most elliptical galaxy nuclei. In addition the abundances read from these models are mostly solar, for ages between 4–16 Gyr (note that this result is logically the same derived from Fig. 4 since metallicity is derived from the same index, i.e. CaT). There are also some outliers, but most of them correspond to data with large error bars in CaT and/or in ⟨Fe⟩. It is clear that most elliptical galaxies fall within the model predictions grid.



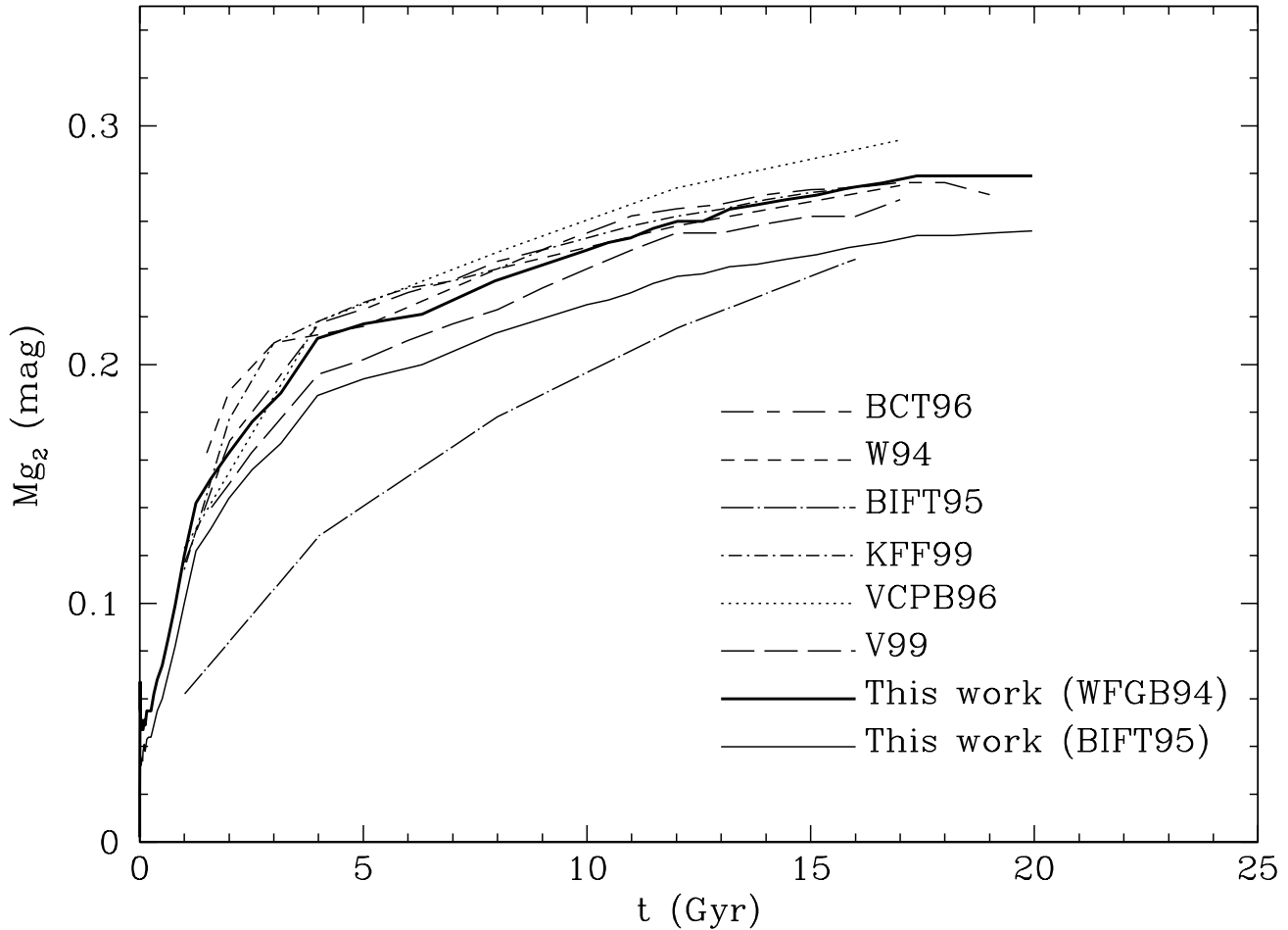


**Fig. 3.** Comparison of the temporal evolution of the  $Mg_2$  index, as predicted by SSP models by different authors and this work.

This diagram confirms the previous trend obtained when comparing  $\langle Fe \rangle$ , with Ca4455 (e.g. Worthey 1998). We conclude then that the simultaneous analysis of Figs. 4 and 5 adds further weight to the idea that calcium follows iron instead of magnesium, reinforcing the observational evidence that calcium and magnesium behave differently in elliptical galaxies (see section 4 for a discussion).

In order to check the possible influence of the extrapolation used on this diagram, we have also shown, as dotted lines, in Fig. 4 and Fig. 5 the results obtained when the empirical equation (1) is used for the stars cooler than 4000. The CaT values are lower but our former conclusions hold: there are a large number of points falling out of the diagram in Fig. 4 while in Fig. 5 some data now fall out but also in the opposite direction.

Other possible error source comes from the uncertainties in the RGB temperature which may be 200 degrees cooler or hotter. We have estimated the effect of a reduction of 200 K in the effective temperature for stars in the RGB on our indices predictions, by indicating these vari-

ations in each figure as an arrow located in a corner of each diagram. This shift is not sufficient to reach the data region in Fig. 4, even using the empirical calibration for the coolest stars.

### 3.2. Disentangling age and metallicity: the CaT- $H\beta$ plane

One of the main problems to understand stellar populations in early-type galaxies is how to disentangle age and metallicity effects. Gonzalez (1993) showed that the combination of the  $H\beta$  line-strength with indices like  $Mg_2$  or  $\langle Fe \rangle$  could break the degeneracy. It is well known that  $H\beta$  is affected by nebular emission. To overcome this problem, higher-order Balmer lines, like  $H\gamma$ , have been proposed as a powerful alternative (Jones and Worthey 1995; Vazdekis and Arimoto 1999). Unfortunately, not many accurate data on this feature have been presented in previous works (but see Kuntschner and Davies 1998). Since the aim of this work is not to derive absolute ages and metallicities but to gather information from the relative

**Table 4.** Line-strength indices for elliptical galaxy nuclei.

Galaxy	CaT	error	Ref.	Mg <sub>2</sub>	error	H $\beta$	error	$\langle$ Fe $\rangle$	error	Ref.	Mg <sub>2</sub>
	(Å)			(mag)		(Å)		(Å)			(mag)
NGC 221	7.60	0.80	(1)	0.216	0.004	2.36	0.05	2.83	0.03	(5)	0.185
NGC 821	6.40	0.80	(1)	0.327	0.004	1.73	0.05	3.04	0.04	(5)	0.304
NGC 1052	8.30	0.80	(1)	0.333	0.007	—	—	2.80	0.15	(11)	0.316
NGC 1700	6.10	0.80	(1)	0.293	0.004	2.09	0.05	3.04	0.04	(5)	0.278
NGC 2693	6.80	0.80	(1)	0.330	0.006	1.17	0.16	2.77	0.21	(9)	0.328
NGC 2778	6.89	0.24	(3)	0.349	0.005	1.76	0.08	2.88	0.05	(5)	0.313
NGC 3115	7.74	0.06	(2)	0.354	0.002	1.80	0.05	3.45	0.08	(10)	0.309
NGC 3377	7.28	0.10	(2)	0.287	0.004	2.07	0.04	2.68	0.03	(5)	0.270
NGC 3379	7.22	0.14	(3)	0.336	0.004	1.65	0.04	2.93	0.03	(5)	0.308
NGC 3608	7.37	0.21	(2)	0.330	0.005	1.73	0.07	2.91	0.04	(5)	0.312
NGC 4261	7.28	0.27	(3)	0.351	0.004	1.43	0.05	3.17	0.04	(5)	0.330
NGC 4278	7.40	0.19	(3)	0.330	0.004	—	—	2.72	0.03	(5)	0.291
NGC 4431	6.95	1.13	(3)	0.184	0.005	1.88	0.20	2.15	0.14	(6)	—
NGC 4458	7.20	0.44	(2)	0.255	0.008	1.62	0.37	2.59	0.35	(8)	0.227
NGC 4472	7.35	0.20	(3)	0.326	0.006	1.72	0.07	3.09	0.06	(5)	0.306
NGC 4478	5.89	0.56	(3)	0.287	0.004	1.87	0.06	2.90	0.04	(5)	0.253
NGC 5845	6.66	0.21	(3)	0.316	0.024	1.63	0.37	2.88	0.40	(8)	0.304
NGC 5846	6.02	0.32	(3)	0.339	0.003	1.60	0.05	2.94	0.03	(5)	0.321
NGC 5846A	7.09	0.40	(3)	0.297	0.002	1.53	0.08	2.61	0.05	(7)	0.287

References for CaT ..... : (1) TDT90  
(2) Deslisle & Hardy 1992  
(3) Gorgas et al. (priv.comm.)

References for blue indices ..... : (4) Worthey et al. 1992  
(5) Gonzalez 1993  
(6) Gorgas et al. 1997  
(7) Pedraz et al. 1999  
(8) GEA90  
(9) Trager et al. 1998  
(10) Fisher et al. 1996 (11) Worthey et al. 1992 for Mg<sub>2</sub>  
and Trager et al. 1998 for H $\beta$  and  $\langle$ Fe $\rangle$   
(12) Davies et al. 1987 for Column (12)

Notes: NGC 1052 and NGC 4278 present H $\beta$  in emission  
NGC 2778 and NGC 4261 present H $\beta$  with emission contamination

trends in the index–index diagrams, we have preferred to use the classical H $\beta$  index, although we note that some particular galaxies may be partially affected by an emission component (see notes in Table 4).

The new model predictions in the H $\beta$ –CaT plane are displayed in Fig. 6. The simultaneous computation of blue and near-IR indices performed in this work allows us to confirm the previous finding of Paper I, already discussed in the introduction to this paper, concerning the orthogonality of the CaT–H $\beta$  diagram and the advantage of this diagram to separate age and metallicity effects. Almost all the data points fall inside the new model predictions, within their error bars. Once again we represent the results obtained through the empirical fit for CaT as dotted lines and an arrow is included in the graph to indicate the possible shift of points if the RGB effective temperature is reduce 200 K.

Taking the models literally, the above diagram indicates that the stellar populations exhibit roughly solar abundances for [Ca/H]. This is naturally the same result obtained from Figs. 4 and 5. In addition, the derived ages range from 4 to 16 Gyr, except for NGC 221, with an age of  $\sim 2$  Gyr, which is not too far from the result derived by Vazdekis & Arimoto (1999), who found that the better fit of a synthetic spectrum to this galaxy is obtained for ages in the range from 2.5 to 5 Gyr. Obviously, these results are not new since they rely on the H $\beta$  indices.

An important problem associated with the use of the Balmer absorption features is that their continuum band-passes usually include metallic lines. Another important drawback, specially in the case of H $\beta$ , is that it is well established that a large fraction ( $\lesssim 50\%$ ) of early-type galaxies exhibit Balmer emission lines at some extent. Therefore, the determination of ages is not totally safe.

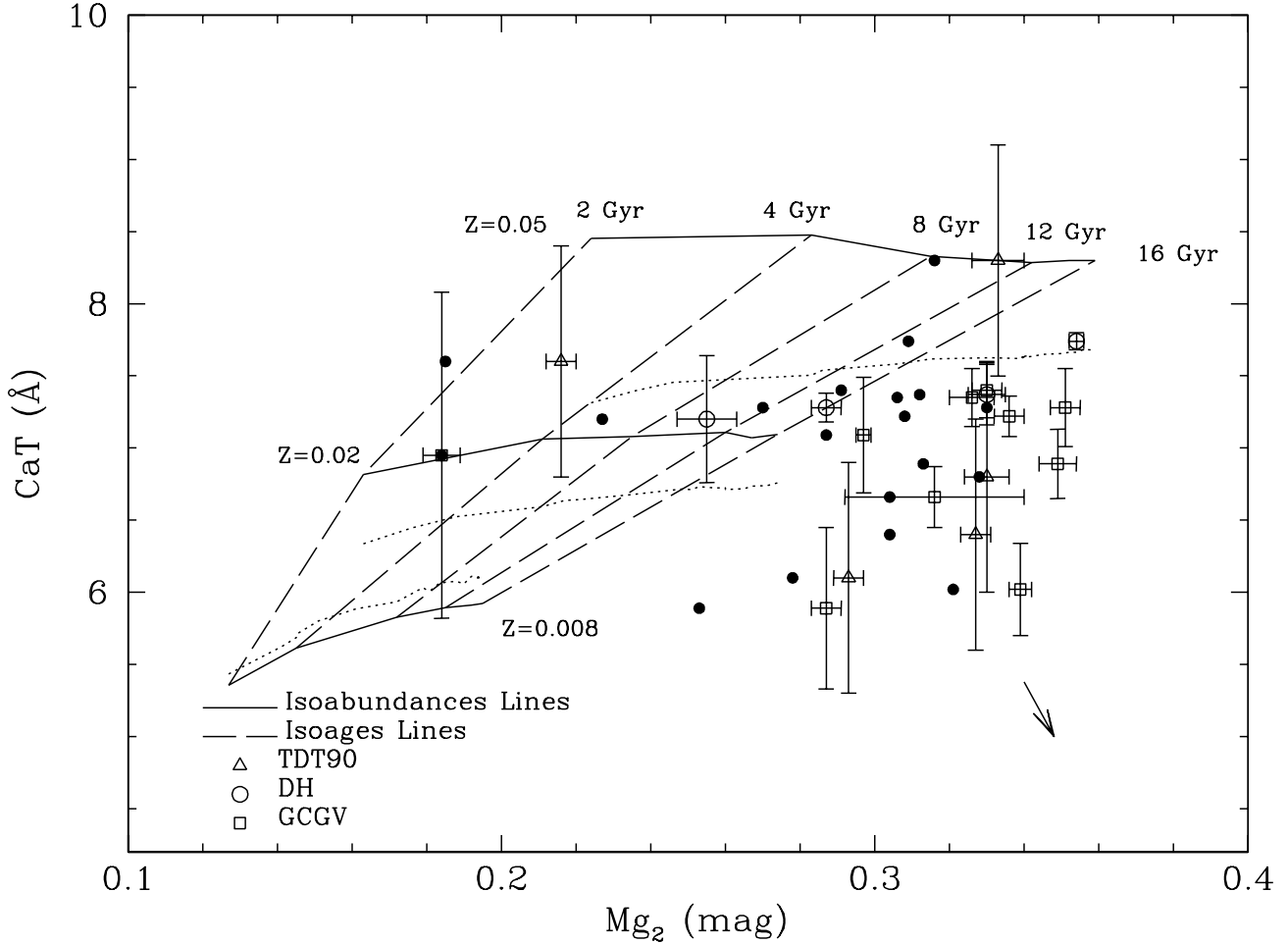


**Fig. 4.** The index CaT vs  $Mg_2$ . Solid lines and long-dashed lines join isoabundance and isoage stellar populations, respectively, as explained in the inset. Dotted lines represent results for isoabundance stellar populations obtained by using the empirical equation (1), instead of the extrapolated theoretical equations JCJ92. Symbols refer to the observational data presented in Table 4: open symbols with error bars refer to  $Mg_2$  from Column (5), while full symbols represent values from Column (12). The small vector on the figure shows the shift of model results which would appear if the effective temperature of the RSG branch was decreased by 200 K.

#### 4. Discussion

As we have already mentioned, a ratio  $[Mg/Fe] > 0$  can be explained by taking into account that both elements are synthesized in the interior of stars covering a different range of stellar masses. Invoking the same reasoning for calcium, it can be concluded that this element is generated in another type of stars than those synthesizing Mg. In this sense, Worthey (1998) has suggested that Type II SNe could have two *flavors*, just like Type I and II SNe produce iron and magnesium at different times in the evolution of a galaxy.

It is important to note that the ratio  $[\alpha/Fe]$  is high because the iron abundance  $[Fe/H]$  is low, i.e., an iron deficiency translates into an over-abundance for alpha-elements. In particular, if one assumes  $[\alpha/Fe]=+0.4$  for a

given total abundance  $Z$ , it means that, for the total abundance  $Z$ ,  $\log Z/Z_{\odot}$  is approximately the same and  $[Fe/H]$  is  $\sim -0.4$  dex smaller. Isochrones do not change very much when alpha-elements are enhanced because abundances of the principal elements are also enhanced; but the iron abundance is decreased (see Tantalo et al. 1998).

The overabundance in  $\alpha$ -elements, or underabundance in  $[Fe/H]$ , which can be seen in the models, occurs because the bulk of the stars are created before the iron is produced. It may be seen when the star formation is low, usually in low-metallicities regions. Thus, the ratio  $[Ca/Fe]$  is over-solar in metal-poor stars (Wallerstein, 1962; Hartmann & Gehren, 1988; Zhao & Magain, 1990; Gratton & Snenen, 1991), such as the  $[Mg/Fe]$  is. This overabundance decreases until solar ratios are reached when the iron abundance increases. For disk dwarfs, Edvardsson et al.

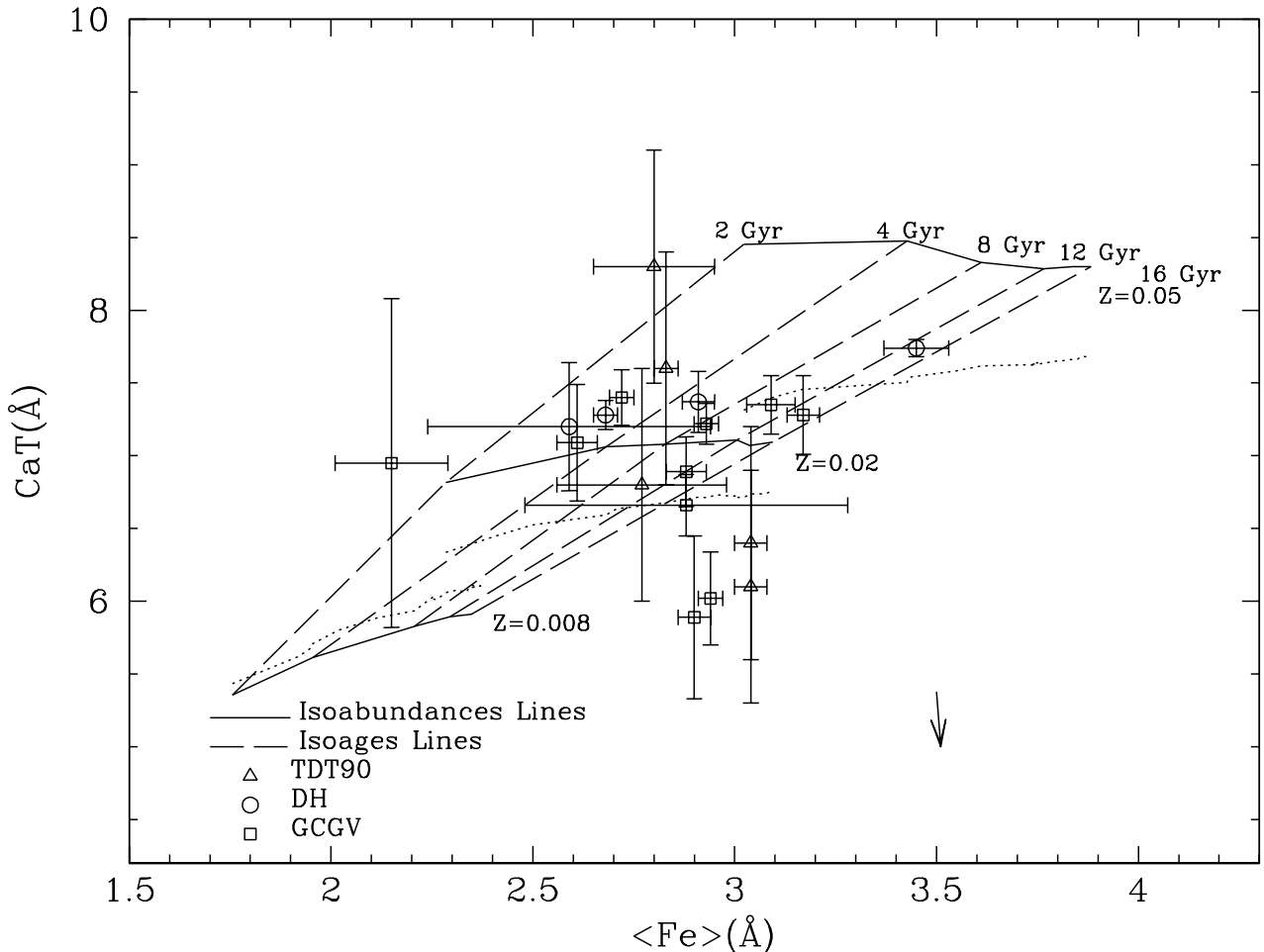


**Fig. 5.** The index CaT vs.  $\langle \text{Fe} \rangle$ , both in  $\text{\AA}$ . The lines and symbols have the same meanings as in previous figures.

(1993). determined the calcium abundances in the range  $-1.0 < [\text{Fe}/\text{H}] < 0.2$  dex, finding that  $[\text{Ca}/\text{Fe}] \sim 0.25$  dex at  $[\text{Fe}/\text{H}] = -1.0$ , and then decreases to solar values just following the magnesium. This kind of behavior may also occur for high metallicities if the time scale for the formation of the bulk of stars is short enough to create stars before the iron appearance,  $\sim 1$  Gyr. McWilliam & Rich (1994) showed, for the Galactic bulge stars, an overabundance in  $[\text{Ca}/\text{Fe}] \sim 0.3$ , slightly lower than those of magnesium and silicon.

Chemical evolution models, including recent theoretical calculations of yields (Timmes et al. 1995), reproduce the Galactic abundances for the so called intermediate alpha-elements (Mg, Si, Ca and Na) as the result of the evolution of the massive stars. (We must note that it is necessary to increase the magnesium yield by a factor of 2 in order to obtain the solar abundance of Mg). Thus the bulk of the star formation should take a time which is shorter than  $\sim 1$  Gyr (the minimum time that has to elapse before the low-mass stars eject the iron in the Type I SNe explosions) in regions where  $[\alpha/\text{Fe}] > 0.0$ ,

and longer for the systems where  $[\text{Mg}/\text{Fe}] = 0.0$ . This result is well reproduced by chemical evolution models (after adequately fitting the data in the solar neighborhood): in Fig. 5 of Molla & Ferrini (1995) we can see a similar behavior for Mg, Ca and Si when stars are formed in a short time scale ( $\sim 0.8$  Gyr).

The fact that  $[\text{Mg}/\text{Fe}] > 0$  in elliptical galaxy nuclei implies that star formation may extend over a time shorter than 1 Gyr. If we now introduce the observed  $[\text{Ca}/\text{Fe}]$  ratio into this reasoning, and we assume that both calcium and magnesium are produced by similar Type II SNe (although with different masses), we can constrain even more the duration of the star formation episode in these regions. In Fig. 7 we represent, simultaneously, the fraction of ejected mass of  $^{24}\text{Mg}$  and  $^{40}\text{Ca}$  over the total yield for each element, taken from Woosley & Weaver (1996), as a function of the stellar mass (lower x-axis) and the mean stellar life (upper x-axis, in logarithmic scale). It is clear from this figure that calcium is produced by stars with mass in the range 12–30  $M_{\odot}$ , while magnesium is generated in stars of 20–40  $M_{\odot}$ . This is in agreement with

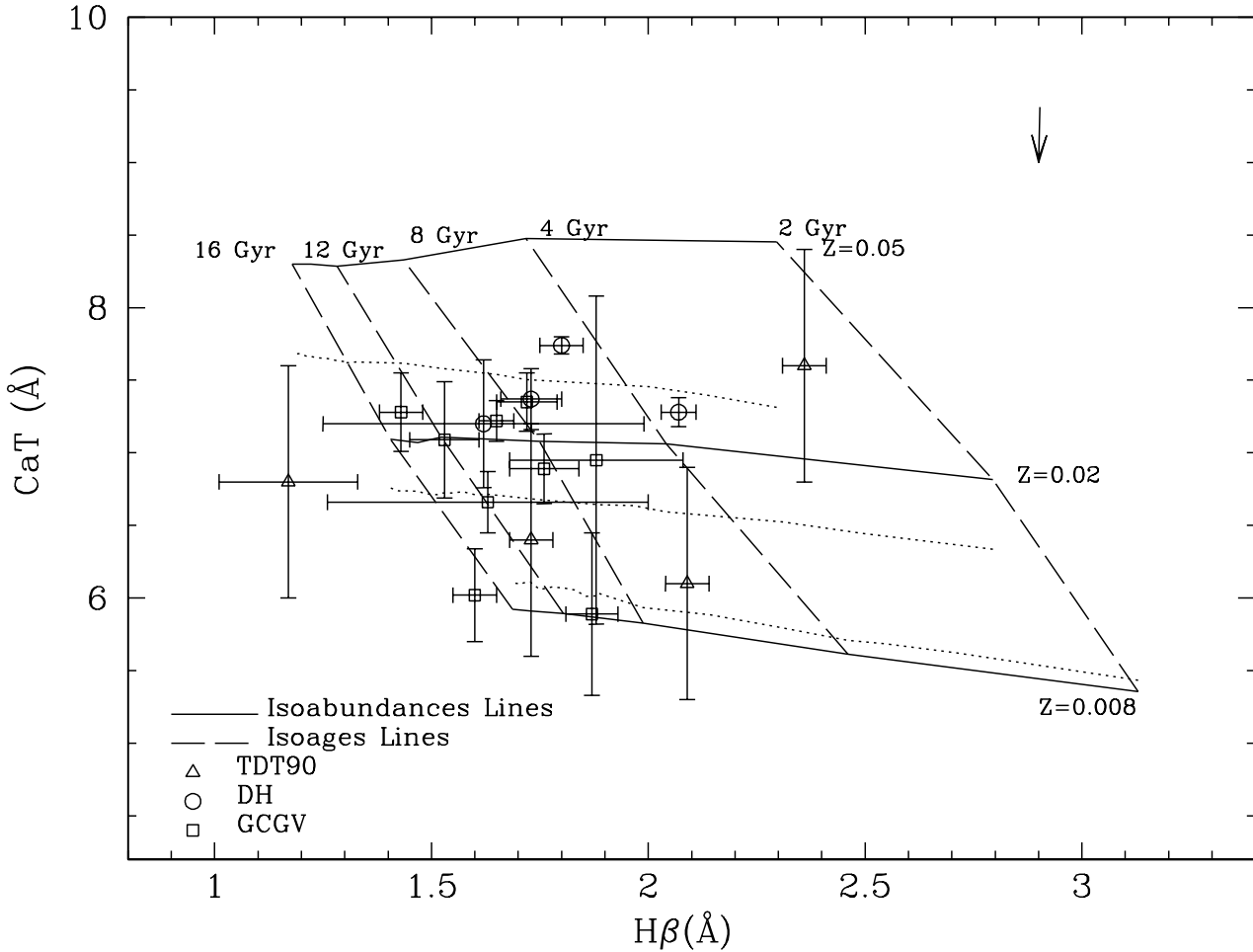


**Fig. 6.** The diagram  $\text{CaT-H}\beta$ . The lines and symbols have the same meanings as in previous figures.

the more recent metallicity-dependent yields from Portinari et al. (1998), who show in their Fig. 4 the ejecta of each element as a function of the CO-core, indicating that calcium proceeds from lower mass stars than those which produce magnesium. Considering the lifetimes of the stars responsible for the bulk production of Ca and Mg, we find these values peak at  $\sim 8.9$  and  $\sim 6.3$  Myr, respectively. Therefore, even with a short difference between both lifetimes ( $\sim 2.6$  Myr), there exists a time period at which the magnesium has already been ejected by the most massive stars but the bulk of the calcium has not yet been released. After this small delay, the calcium appears in the ISM, and stars formed afterwards will incorporate both elements, Mg and Ca, showing  $[\text{Mg}/\text{Fe}]$  and  $[\text{Ca}/\text{Fe}]$  larger than zero and a ratio  $[\text{Mg}/\text{Ca}]$  tending to solar.

The consequence of this reasoning is important: if in elliptical galaxy nuclei calcium is not over-abundant, while magnesium is, their stellar populations could have been formed, at least *locally*, in a very short burst, lasting a

timescale smaller than a few Myr.<sup>2</sup> If the star formation took more than this time, the calcium would have been incorporated into the new stars, and one should expect to observe  $[\text{Mg}/\text{Ca}] \simeq 0$ , which does not seem to be the case. This is in agreement with the dissipative theory of galaxy formation where the collapse time scale must be shorter for more massive galaxies by producing a correlation between the time scale of the star formation in these galaxies and the total mass. This is supported by Richer et al. (1998), who claim that  $[\text{O}/\text{H}]$  varies systematically with the velocity dispersion for spheroidals, bulges and ellipticals, by relating the gravitational potential well with this effect and by concluding that the time scale governs  $[\text{O}/\text{Fe}]$  or  $[\text{Mg}/\text{Fe}]$ . The result implies a short time scale for star formation in more massive elliptical and bulges,

<sup>2</sup> A word of caution must be said when considering the speed of the star formation in a stellar system. The quoted times always refer to *local* times, i.e. those needed to produce the bulk of the star formation locally, although the required times to form the whole system, for instance a galaxy, could be much larger.

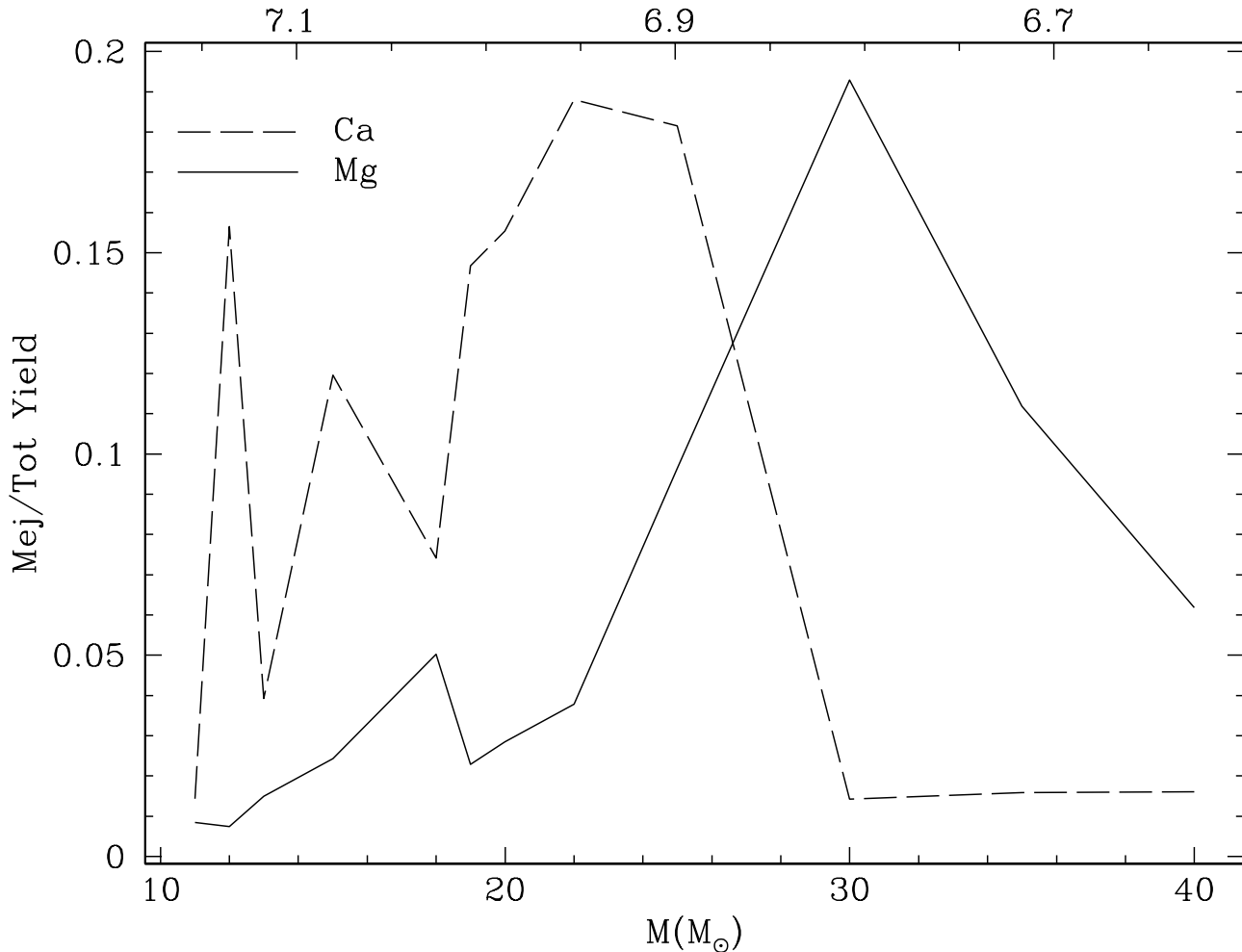


**Fig. 7.** Magnesium and calcium yields taken from Woosley & Weaver (1995) as a function of the stellar mass (lower x-axis) and mean stellar life (upper x-axis, years in logarithmic scale).

supporting the old idea that ellipticals are simpler than low mass galaxies from their star formation history.

However, the deduced constraint for the local star formation time might seem to be too short. Then a new scenario, which could include the two Type II SNe *flavors*, must be invoked. This effect can also be enhanced (or even dominated) by a flatter initial mass function due to special conditions (dense environment or high metallicity). If an IMF is biased towards massive stars, the magnesium produced or *yield* in these elliptical nuclei will be larger, allowing one to find overabundances of magnesium and also of other elements ejected by the most massive stars such as oxygen, but not of those ejected by less massive stars. An IMF universal and constant is still a matter of discussion (Larson 1998, Padoan et al. 1997, Meyer et al. 1999, Chiosi et al. 1998), but some recent works claim that it must be constant (Wyse 1997, Tsujimoto et al. 1999, Chiappini et al. 1999).

One point that may enlighten this problem proceeds from the nucleosynthetic yield calculations: by using the

existing yields in a chemical evolution model, it is not possible to reproduce the solar abundance  $[Mg/H]$ . It is necessary to add magnesium to the stellar production to reach the estimated solar value. The quantity of ejected magnesium must be a factor of  $\sim 2$  greater than the present yield, implying that Fig. 7 must change. If the deficiency in magnesium might be accounted for by the production of the most massive stars ( $M > 40M_{\odot}$ ), we might solve two problems: chemical evolution models would reproduce the solar abundances and the difference between stellar lifetimes for stars producing Mg and Ca would be large enough to allow the formation of stellar populations with an overabundance  $[Mg/Ca]$  in a sufficient time.

Another possible solution to this problem, besides the actual ratio  $[Mg/Fe]$  non solar, may be related with the measures of  $Mg_2$  as we see by comparing columns (12) and (5) from Table 4. For some galaxies there exist data from different authors and there are differences as large as 0.05, that is, 15 %. Following Goudfrooij & Emsellem (1996) the possible emission lines may affect the measures

of absorption lines. They estimated that the index Mg<sub>b</sub> may be artificially enhanced by 0.4-0.1 Å and Mg<sub>2</sub> by 0.03 mag, due to the [N I] emission-line doublet at 5199 Å. Taking into account that 50 % of giant elliptical galaxies exhibit H $\alpha$ + [N II] emission, maybe the actual Mg<sub>2</sub> values must be reduced. If we reduce the Mg<sub>2</sub> data by 15 %, most of them might be almost reproduced by models, as we show in Fig. 4 where the two sets of data (open vs full) are represented.

In this context, a surprising result has been obtained by Origlia et al. (1997). These authors have measured the strength of the infrared absorption line at 1.59  $\mu$ m, which is primarily sensitive to the total silicon abundance. These authors used this absorption to estimate the ratio [Si/Fe] necessary to reproduce their EW, by comparing a sample of elliptical galaxies and globular clusters with models. They found that silicon could be enhanced by about 0.5 dex in both kinds of stellar systems. Since Si and Ca proceed from stars with similar masses (Portinari et al. 1998), both should be overabundant at the same time, contrary to our and their findings and to our explanations for the existence of an overabundance in [Mg/Ca]. Thus, the question remains unclear until more precise calculations of nucleosynthesis yields and observations of alpha-elements become available.

## 5. Conclusions

We have developed an evolutionary synthesis model with which we have produced a grid of models for SSP at 6 metallicities and a wide age range. This code is able to predict indices in the blue-visible spectral range, the classical *Lick* indices and indices in the near-IR such CaT, Mg I and Na I at the same time.

We have carefully analyzed the behavior of this index for the coolest stars ( $T_{\text{eff}} < 4000$ ), given by some samples of data available in the literature, obtaining the generic trend of CaT decreasing with effective temperature, in agreement with the extrapolated JG92's theoretical functions. Therefore, although systematic effects may still be present in the theoretical predictions, mainly due to potential errors in the extrapolation of these JG92 equations, we use the most adequate solution until more reliable fitting functions become available.

We have compiled a set of data from the literature for galaxies for which both kind of indices, blue-visible and near-IR, had been observed, and we have compared their predictions with data.

We have used our results to study the relationship between different indices for old stellar populations by producing diagnostic diagrams in which observed data and models can be plotted to determine the basic physical properties of the dominant stellar population in these galaxies. We find that most of the galaxies with known data for Mg<sub>2</sub>, CaT and  $\langle \text{Fe} \rangle$  remain in the CaT - Mg<sub>2</sub> plane at the place of  $Z=0.02$ , while they seem to have

overabundances of Mg. This conclusion is in agreement with other data of Ca4300 in the blue region found by Worthey (1998), but raises the question of how it is possible to have solar metallicity ratio for the calcium element and over-solar ratio for Mg abundance, while both are  $\alpha$ -element produced by the same type of massive stars.

If we accept the assumption of a relative abundance  $[\text{Mg}/\text{X}] > 0$ , adopted to explain this kind of diagram and that it is due to a short time scale for the star formation, and we apply the same argument for the [Mg/Ca], this would imply that the star formation time scale in elliptical galaxy nuclei must be shorter than  $\sim 5 - 10$  Myr. Otherwise, we should not find a discrepancy between the data and the models in the later diagnostic, where both indices proceed from the same kind of alpha-elements, which is not the case. We suggest that an update of the nucleosynthesis yields of Mg, increasing the production of Mg for the more massive stars, may solve this problem, by extending the elapsed time between the production of Mg and of Ca and, in consequence, the time scale for the star formation. An alternative explanation might be an IMF biased towards the massive stars ( $M > 40M_{\odot}$ ) in the early phases of star formation in elliptical galaxies.

We must keep in mind that the emission over these spectra also may affect Mg<sub>2</sub> data: they may be reduced by 5 % if a careful analysis is done before obtaining the spectral indices Mg<sub>b</sub> and Mg<sub>2</sub>.

We use the orthogonal diagram CaT - H $\beta$  to date elliptical galaxies and to determinate their abundances, reaching the conclusion that elliptical galaxies are nearby solar in their abundances of calcium, in the same way as for iron, and that their ages range between 8 -16 Gyr.

A large campaign of observations in the near-infrared to estimate the CaT index, e.g. in the same set of galaxies given in Davies et al. (1987), would be very useful to date them and to determinate their metallicities/abundances in a clear way.

*Acknowledgements.* We thank J. Gorgas and N. Cardiel for the permission to use their CaT data before publication and for fruitful discussions. We are grateful to Sonya Delisle and Eduardo Hardy who kindly sent us their spectra in the red bandpass. We thank the referee, Guy Worthey, for his useful comments for the improvement of this paper. We also thank A. I. Díaz for suggestions in the final version of this work and J. Gea Banacloche for the help in the english version. M.M. thanks the Université Laval (Quebec) for the nice period, during which part of this work was done. M.M. has been supported by a post-doctoral fellow of the Spanish *Ministerio de Educación y Cultura*. This work has made use of the NASA Astrophysics Data System.

## References

- Borges, A.C., Idiart, T.P., de Freitas-Pacheco, J.A., & Thevenin, F. 1995, AJ, 110, 2408 (BIFT95)
- Bressan, A., Fagotto, F., Bertelli, G., Chiosi, C. 1993, A&AS, 100, 647

- Bressan, A., Chiosi, C., & Tantalo, R. 1996, A&A, 311, 425 (BCT96)
- Burstein, D., Faber, S.M., Gaskell, C.M., & Krumm, N. 1984, ApJ, 287, 586
- Casuso, E., Vazdekis, A., Peletier, R., & Beckman, J.E. 1996, ApJ, 458, 533
- Carollo, M., & Danzinger, I.J. 1994a, MNRAS, 270, 525
- Carollo, M., & Danzinger, I.J. 1994b, MNRAS, 270, 743
- Chiappini, C., Matteucci, F., & Padoan, P. 1999,
- Chiosi, C., Bressan, A., Portinari, L., & Tantalo, R. 1998, A&A, 339, 355
- Clegg, R.E.S. & Middlemass, D. 1987, MNRAS, 228, 759
- Davies, R.L., Burstein, D., Dressler, A., Faber, S.M., Lynden-Bell, D., Terlevich, R., & Wegner, G. 1987, ApJS, 64, 581
- Davies, R.L., Sadler, E.M., & Peletier, R.F. 1993, MNRAS, 262, 650
- Deslisle S., & Hardy, E. 1992, AJ, 103,711 (DH)
- Díaz, A.I., Terlevich, E., & Terlevich R. 1989, MNRAS, 239, 325 (DTT)
- Edvardsson, B., Andersen, J., Gustafsson, B., Lambert, D.L., Nissen, P. E., & Tomkin, J. 1993, A&A, 275, 101
- Fisher, D., Franx, M., & Illingworth, G. 1996, ApJ, 459, 110
- García-Vargas, M.L., Bressan, A., & Díaz, A.I. 1995, A&AS, 112, 13
- García-Vargas, M.L., Mollá, M. & Bressan, A. 1998, A&AS, 130, 513, Paper I
- Gonzalez, J.J. 1993, Ph Thesis, Univ. California, Santa Cruz
- Gorgas, J., Efstathiou, G., & Aragón-Salamanca, A. 1990, MNRAS, 245,217 (GEA90)
- Gorgas J., Faber S.M., Burstein D., González J.J., Courteau S. & Prosser C. 1993, ApJS, 86, 153
- Gorgas, J., Pedraz, S., Guzmán, R., Cardiel, N., & Gonzalez, J.J. 1997, ApJ, 481, L19
- Gorgas, J., Cardiel, N. & García-Vargas, M.L. *private communication*(GCGV)
- Groth R. G., & Sneden, C. 1991, A&A, 241, 501
- Gudfrooij, P. & Emsellem, E. 1996, A&A, 306, L45
- Hartmann, K., & Gehren, T. 1988, A&A, 199, 269
- Henry, R. B. C. & Worthey, G. 1999, PASP, 111, 919
- Idiart T. P., & Freitas-Pacheco, J. A. 1995, AJ, 109, 2218
- Idiart T. P., Thevenin, F., & Freitas-Pacheco, J. A. 1996, AJ, 113, 1066
- Jones L.A. & Worthey G. 1995, ApJL, 446, 31
- Jørgensen U.G., Carlsson M. & Johnson H.R. 1992, A&A, 254, 258 (JCJ92)
- Kuntschner, H., & Davies, R.L. 1998, MNRAS, 259, L29
- Kurth, O.M., Fritze-v.Alvensleben, U., & Fricke K.J. 1999, A&AS, 138, 19
- Larson, R. B. 1998, MNRAS, 301, 569
- Leitherer, C., Alloin, D., Fritze-v. Alvensleben, U., et al 1998, PASP, 108, 1017
- Lejeune, T., Cuisinier, F., & Buser, R. 1997, A&AS, 125, 229
- Lejeune, T., Cuisinier, F., & Buser, R. 1998, A&AS, 130, 65
- Mallik, S. V. 1997, A&AS, 124, 359
- Mayya, Y.D. 1997, ApJ, 482, L149
- McWilliam A., Rich R.M., 1994, ApJS, 91,749
- Meyer, M. R., Adams, F. C., Hillenbrand, L. A., Carpenter, J. M., & Larson, R. B. 1999, in Protostars & Planets, Eds. V. Manning, A. Boss, & S. Russell (Tucson: the University of Arizona Press), in press.
- Mollá, M., Ferrini, F., 1995, ApJ, 454,726
- Mollá, M., Ferrini, F., Hardy, E., & García-Vargas, M.L. 2000, A&A, submitted.
- Origlia, L., Ferraro, F. R., Fusi Pecci, F., & Oliva, E. 1997, A&A, 321, 859
- Padoan, P., Nordlund, A., Jones, B. J., T. 1997, MNRAS, 288, 145
- Pedraz, S., Gorgas, J., Cardiel, N., & Guzman, R., 1999,
- Pellerin, A., & Robert, C. 1999, in Spectrophotometric Dating of Stars and Galaxies, ASP Conf. Ser. 192, Eds. I. Hubeny, S.R. Heap & R.H. Cornett, p. 57.
- Portinari, L., Chiosi, C. & Bressan, A 1998, A&A, 334, 505
- Richer, M. G., McCall, M.L., Stasińska, G., 1998, A&A, 340, 67
- Schiavon, R. P., Barbuy, B., & Bruzual, A. 1999, ApJ, accepted, (SBB99)
- Tantalo, R., Chiosi, C., & Bressan, A. 1998, A&A, 333, 419
- Terlevich, E., Díaz, A.I., & Terlevich R. 1990, MNRAS, 242, 271 (TDT90)
- Timmes, F. X., Woosley, S. E., & Weaver, T. A. 1995, ApJS, , 98, 617
- Trager, S. C., Worthey, G., Faber, S.M., Burstein, D., & González, J.J. 1998, ApJS, 116, 1
- Tsujimoto, T., Shigeyama, T., & Yoshii, Y. 1999, ApJ, 519, L63
- Vazdekis, A. 1999, ApJ, 513, 224
- Vazdekis, A. & Arimoto, N. 1999, ApJ, 525, 144
- Vazdekis A., Casuso E., Peletier R.F. & Beckman J.E. 1996, ApJS, 106, 307
- Vazdekis A., Peletier R.F., Beckman J.E., & Casuso E. 1997, ApJS, 111, 207
- Wallerstein, G. 1962, ApJS, 6, 40
- Weiss, A., Peletier, R. F. & Matteucci, F. 1995, A&A, 296, 73
- Wyse, R. F. G. 1997, ApJ, 490, L69
- Woosley, S. E., & Weaver, T. A. 1995, ApJSS, 101, 181
- Worthey, G. 1994, ApJS, 95, 107
- Worthey, G. 1998, PASP, 110, 888
- Worthey, G., Faber, S.M., & Gonzalez J.J. 1992, ApJ, 398, 69
- Worthey, G., Faber, S.M., Gonzalez J.J., & Burstein, D. 1994, ApJS, 94, 687
- Worthey, G. & Ottaviani, D. L. 1997, ApJS, 111, 377
- Zhao, G. & Magain, P. 1990, A&AS, 86, 85
- Zhou, X. 1991, A&A, 248, 367
- Zhu, Z. X., Friedjung, M., Zhao, G., Hang, H. R., & Huang, C. C. 1999, A&AS, 140, 69